Cell Calcium 53 (2013) 231–240

Contents lists available at SciVerse ScienceDirect

Cell Calcium

journal homepage: www.elsevier.com/locate/ceca

Analysis and regulation of amoeboid-like cell motility using synthetic Ca^{2+}-sensitive proteins

Evan Mills[a], Kevin Truong[a,b,*]

[a] Institute of Biomaterials and Biomedical Engineering, University of Toronto, 164 College Street, Toronto, Ontario, M5S 3G9, Canada
[b] Edward S. Rogers Sr. Department of Electrical and Computer Engineering, University of Toronto, 10 King's College Circle, Toronto, Ontario, M5S 3G4, Canada

ARTICLE INFO

Article history:
Received 31 August 2012
Received in revised form
18 December 2012
Accepted 24 December 2012
Available online 23 January 2013

Keywords:
Cell motility
Ca^{2+} networks
RhoA
Blebbing

ABSTRACT

Several recent reports have demonstrated how engineered proteins can control cell motility, an important functional module for ultimately programming cells as therapeutics. We have reported two engineered proteins that regulate the blebbing cell morphology using chimeras of RhoA, a protein that regulates cytoskeletal tension. Here, we show that engineered switching of blebbing can be used to regulate cell motility. First, the analysis of morphology and motility characteristics showed that blebbing cells wobbled, or shifted, faster and less linearly than cells with a wild type morphology. Second, activating engineered protein switches that regulate cell morphology led to predictable changes in motility characteristics. Last, exogenous stimuli such as blue light, acetylcholine and VEGF-A were used to show that groups of proteins could cooperatively increase cell motility *in vitro*. This work demonstrates that control of RhoA can program the motility patterns of living cells and has implications in studying the relationship between cell morphology and motility.

1. Introduction

Mammalian cells are versatile, robust biochemical entities that execute a wide range of physiological functions including migration, programmed death, phagocytosis and protein secretion. The disruption of genetic and protein networks within the cell are often the cause of disease, and standard disease therapies often involve surgical intervention or delivering small molecules or proteins, produced *in vitro*, to the cell. Several studies have recently reported using mammalian cells as therapeutic platforms, whether it be by modifying a diseased cell itself [1] or "programming" therapeutically relevant cells such as T-cells [2] or hematopoietic stem cells [3] with novel, useful functions. While such studies are relatively rare, in our view this may eventually lead to the use of the mammalian cells as a standard, customizable therapeutic platform, not unlike the current view of nanoparticles [4], engineered viruses [1] and biomaterials [5]. Such an application for mammalian cells is relatively unexplored, but in principle they offer several inherent advantages such as being able to support large genetic networks [6], the ability to be drawn from a host or patient [2], therefore limiting unwanted immunological interactions, and having the inherent ability to migrate, secrete proteins and fuse membranes. Several disadvantages of using mammalian cells for therapy include their complexity, heterogeneity and their strict handling requirements *in vitro* or *ex vivo*.

In the long-term, the successful development of mammalian cells as therapeutic platforms will require the combination of well-defined modules that direct useful physiological functions (for example, directed migration, protein secretion, gene delivery, *etc.*) to perform complex tasks (for example, seeking and destroying populations of tumor cells). Cell migration is one such basic module that may be useful in several potential applications, and several chimeric proteins, based on Rho proteins [7], have been reported to regulate cell migration and the cytoskeleton [8–14]. Some of the reported chimeras have been designed such that cells migrate in response to light [9,13], but this control signal may not be easily translated to large organisms due to light's poor tissue penetration. Instead, chemical, mechanical or physical cues that can operate *in vivo* in large organisms will allow more autonomous migration based on disease-related cues such as the secretion of growth factors from tumor cells. Reported photoactivatable systems cannot be readily altered to respond to chemical or other stimuli because they were developed using specific allosteric [13] or binding [9] interactions between light-sensing proteins and Rho GTPases.

Recently, our lab has reported two RhoA chimeras that can regulate cell morphology in response to a variety of exogenous stimuli including ATP, acetylcholine (ACh) and blue light [10,11]. In these chimeras, RhoA and its kinase, ROCK, were responsible for switching the blebbing morphology in a variety of standard cell lines.

* Corresponding author at: Institute of Biomaterials and Biomedical Engineering, University of Toronto, 164 College Street, Toronto, Ontario, M5S 3G9, Canada. Tel.: +1 416 978 7772; fax: +1 416 978 4317.
E-mail addresses: e.mills@mail.utoronto.ca (E. Mills), kevin.truong@utoronto.ca (K. Truong).

0143-4160/$ – see front matter © 2013 Elsevier Ltd. All rights reserved.
http://dx.doi.org/10.1016/j.ceca.2012.12.005

Blebs are dynamic, quasi-spherical protrusions that result from detachment of the plasma membrane (PM) from the underlying cytoskeleton when RhoA/ROCK activation leads to actin-myosin crosslinking and an increase in cytoskeletal tension [15,16]. We achieved control over blebbing in response to a diverse set of external stimuli by using the Ca^{2+} second messenger [17] as an intermediate signal. External stimuli activated their respective Ca^{2+}-mobilizing domains [18–20], generating local Ca^{2+} increases that activated our Ca^{2+}-sensitive chimeras. In particular, the fusion protein CaM-RhoA(DP), a tandem fusion of calmodulin (CaM) and dominant positive (DP) RhoA, establishes the blebbing morphology at basal Ca^{2+} concentrations, and signals which elevate Ca^{2+} result in bleb retraction [10]. Conversely, the chimera CaRQ, a fusion of CaM and RhoA(DP) with artificially and rationally-chosen embedded CaM-binding peptides, has no effect on cell morphology at basal Ca^{2+}, but with elevations in local Ca^{2+} at the PM, CaRQ is activated and causes blebbing [11].

The blebbing morphology has been linked to cell migration, sometimes called "amoeboid-like cell migration" in several contexts, including *Danio Rerio* germ cell development [21,22], some modes of leukocyte migration [23] and the migration and invasion of certain metastatic cancer cells [24,25]. The migration mode of a particular cell may be amoeboid-like, mesenchymal (based on Rac1 and Cdc42-directed actin polymerization at the leading edge) [26–29], or some combination of the two. In the case of blebs leading to amoeboid-like migration, as the bleb expands, cytosol rushes to fill the new space causing the cell to "tumble" forward [21]. As a bleb ages over 1–2 min, actin polymerizes inside the bleb re-linking the PM with the cytoskeleton [30]. This has two effects: first, it enables transmembrane adhesion receptors such as E-cadherin to anchor the bleb to the extracellular matrix or neighboring cells, allowing the cell to realize forward movement from the "tumble" [22], and second, retracts the bleb. A subsequent bleb in an area near the first one will allow the cell to continue to move in the same direction. Many *in vitro* studies quantify cell migration by examining single cells or with population-level assays. In single cell studies, individual cells are tracked by time-lapse microscopy, tracks are often reconstructed [22,31,32] and analyzed for the speed, linearity and coherence of migration [31]. At the population level, a variety of assays have been used to quantify migration in response to chemical cues, pharmacological agents and substrate properties, including scratch wound [33–35], transwell [36–38] and invasion assays [25,39].

Here, we show that cell migration can be switched by regulating the blebbing morphology using the engineered protein chimeras CaM-RhoA(DP) and CaRQ. Single-cell tracking analysis and population-based transwell assays are used to show that the linearity, speed and directionality of motile and migrating cells can be switched in response to a variety of extracellular stimuli including light, ACh and vascular endothelial growth factor (VEGF-A). This demonstrates that engineered protein systems can be used in a modular way to control cell migration, a step toward programming cells for therapeutic applications. Throughout, we use the term motility to describe the characteristic of a cell to exhibit short term shifts or wobbles in its position [16,40], as defined by its centroid, the magnitude of which may be less than a cell width, and migration to describe long-term changes in position that are large relative to the size of the cell.

2. Methods

2.1. Cell culture and transfection

HEK293 cells were maintained in Dulbecco's Modidified Eagle's Medium supplemented with 25 mM D-glucose, 1 mM sodium pyruvate and 4 mM L-glutamine (Invitrogen, Carlsbad, CA) in a T-25 flask, maintained in a 37 °C incubator with 5% CO_2. Cells were passaged at 95% confluency using 0.05% trypsin with EDTA (Sigma–Aldrich, St. Louis, MO) and seeded onto glass-bottom dishes at 1:15 dilution for transfection (Mattek, Ashland, MA). Cells were transiently transfected using Lipofectamine 2000 according to manufacturer's directions (Invitrogen).

2.2. Reagents used

Cells treated with Y-27632 (5 μM), blebbistatin (10 μM) and CDZ (50 μM) were pre-incubated with inhibitor in PBS with $CaCl_2$ for 1 h prior to imaging. ACh (1 mM), ionomycin (1 μM) and VEGF-A (10 ng/mL from Cell Signaling Technologies, Pickering, Canada) were added by diluting 1:10 into imaging medium (PBS with $CaCl_2$, except where noted otherwise). All reagents, except where noted, were from Sigma.

2.3. Imaging

Imaging was performed using an inverted IX81 microscope with Lambda DG4 xenon lamp source and QuantEM 512SC CCD camera with a 20× or 60× oil immersion, or 10× objectives (Olympus, Markham, ON, Canada). Filter excitation (EX) and emission (EM) bandpass specifications were as follows (in nm): for CFP EX: 438/24, EM: 482/32; for YFP EX: 500/24, EM: 542/27; for RFP EX: 580/20, EM: 630/60 (Semrock, Rochester, NY, USA). For LOVS1K, excitation was done using the CFP excitation filter normally with a 300 ms flash every 10 s.

2.4. Single-cell migration assay

For experiments where single cell migration characteristics were observed (Figs. 1–3), cells were trypsinized after transfection and re-seeded at 1:10 dilution onto Mattek glass-bottom dishes in DMEM + 1% FBS and allowed to attach for 4 h before imaging. Images were captured every 5 s during the imaging window. After the experiment, stacks of images were thresholded such that the background, any debris, and the majority of the image representing the bleb itself were excluded (so that the bleb protrusion did not skew the subsequent centroid calculation). The centroid of the cell particle was calculated over time using ImageJ plugin "Analyze Particles". Cells which detached partway through the experiment, moved out of the image frame, or spontaneously rounded and shrank were excluded from the analysis. Linearity and speed were calculated as described in Section 3.

2.5. Transwell assay

24 h before cell seeding, inserts were soaked in 100 μL complete growth medium and cells were passaged and transfected as described above. On the day of seeding, the incubating medium was removed from the inserts, cells were detached from their transfection culture dishes by trypsin, and seeded onto the inserts in 100 μL DMEM + 1% FBS, with any inhibitors, in a 1:30 dilution (to match the reduction in area from 6-well plate format to the insert membrane area) to the apical chamber. The same volume of cell suspension was seeded in a well without insert as the positive control. The basal chamber was then loaded with 650 μL DMEM + 1% FBS, with any inhibitors or chemoattractants.

For illumination, 24-well plates were placed, in a dark incubator, on an iPod 3G that was programmed to display a blue screen such that when a 24-well plate was placed on top of the iPod, cells in the wells would be exposed to blue light (1 mW/cm^2 power output, compared to 25 mW/cm^2 on the microscope stage). Based on

published transmission efficiencies and the geometry of the transwell system, we estimate that approximately 33% of the output power was able to reach the cells on the opposite site of the transwell filter [52]: 78% transmission of 445 nm light through 1 mm of each polsytrene culture dish and filter insert, and 55% transmission of 445 nm light through 5 mm of DMEM + FBS (actual depth was closer to 2 mm, so the overall estimate is conservative). Conditions requiring darkness were loosely wrapped in aluminum foil.

After 24 h the transwell insert was removed from the basal chamber and excess cells were removed from the apical layer by cotton swabs. The insert was then soaked in PBS and then trypsin for 30 min to detach cells on the basal side of the insert. Images were taken of 5 random fields (10× objective) from the receiver, PBS and trypsin wells of each insert after 1 h incubation to allow for settling. The average of the 5 images, summed over the three wells per condition, was divided by the same condition from the control well to determine the migration index. Each experimental condition was performed in triplicate.

2.6. Data analysis

For single-cell migration characteristics, the data is the mean of at least 10 cells and the error bars are the SEM. For transwell and VEGFR2 characterization experiments, the data is the mean of 3 independent experiments and the error bars are the SEM unless otherwise noted. Significance, where discussed, was determined using paired or unpaired Student's *t*-tests (as appropriate, depending on the context). For cases where more than 2 conditions were presented in the same graph (*e.g.* Fig. 1E), the Sidak correction was used and *P* values stated in the figure and text were updated to include the transformation below where *m* is the number of conditions presented in the graph:

$$P_{Corrected} = 1 - (1 - P_{Uncorrected})^{m-1}$$

3. Results

3.1. Blebbing cells have distinct single-cell motility characteristics

Cells that were dynamically forming and retracting blebs showed different motility patterns, or tracks than cells with a wild type morphology (Fig. 1A–C and Movies 1–3). Throughout, we consider a bleb to be a mostly spherical protrusion from the cell body, that is dynamically formed and retracted on the order of 1–2 min [30,41]. Cell centroid tracks were reconstructed after 2 h of time-lapse microscopy of freshly seeded HEK293 cells (see Section 2 for more details). Three different cases were studied: cells that were blebbing because they were overexpressing CaM-RhoA(DP), where RhoA is inactivated by Ca^{2+}, and apparently wild type morphology cells overexpressing YFP or CaRQ, where RhoA is activated by Ca^{2+}. Blebbing cells (overexpressing CaM-RhoA(DP)), appeared to shift the location of their centroids faster than cells with apparently wild type morphology (overexpressing YFP or CaRQ), but without necessarily larger overall displacement. The tracks tended to be more jagged, compact and non-linear for blebbing cells (Fig. 1B) than others (Fig. 1A and C).

Supplementary data related to this article found, in the online version, at http://dx.doi.org/10.1016/j.ceca.2012.12.005.

Speed and linearity have been used by others [31] to characterize single cell motility. Speed, or distance traveled over time, is a familiar quantity not to be confused with velocity which is displacement over time. Linearity refers to the quality of a cell moving in a straight line, and can be quantified as the ratio of distance traveled to displacement in a given time window (Fig. 1D). Linearity can therefore range from 1 (following a straight line) to 0 (where a cell with non-zero path length starts and stops at the same point).

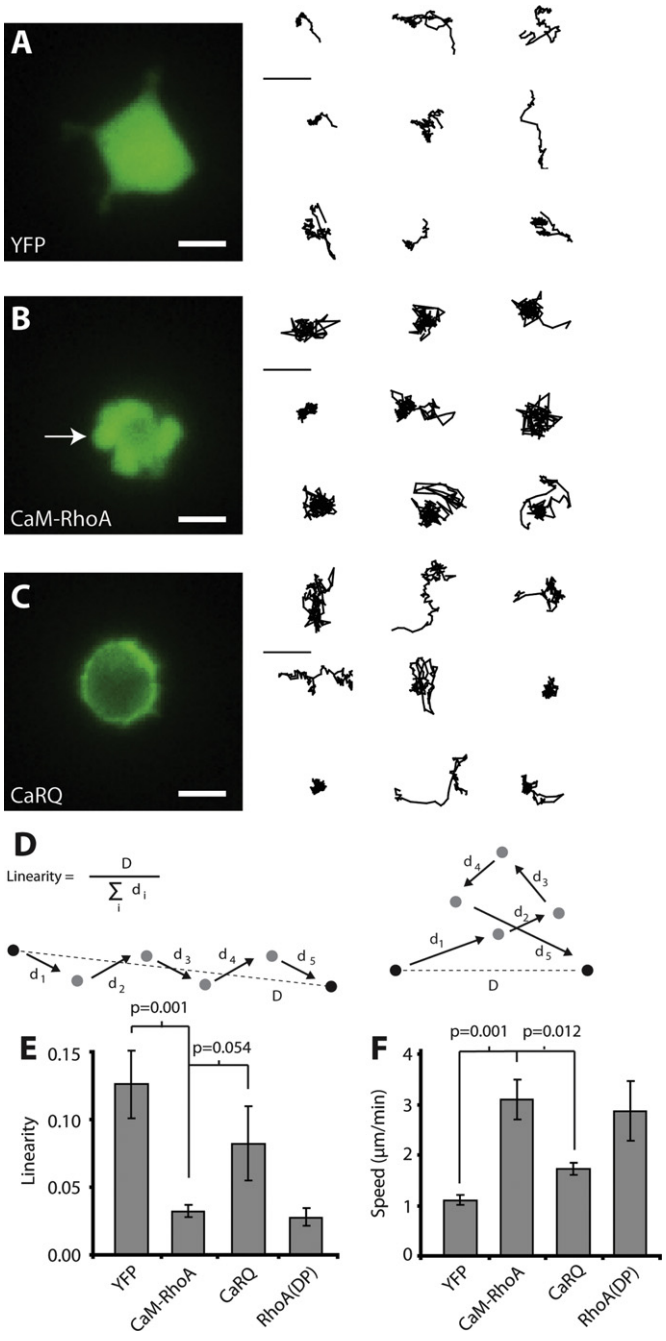

Fig. 1. Comparison of motility characteristics based on cell morphology. (A–C) Representative images of cells (left) with a set of tracks (right) recorded over 2 h (A: YFP, B: CaM-RhoA, C: CaRQ). Scale bars are 20 μm in images and 10 μm in tracks. YFP channel is shown for each case. (D) Cartoons of linearity calculation for a cell moving more linearly (left) and less linearly (right) over 5 time points. (E, F) Summary of linearity and speed quantified for cells overexpressing the indicated fluorescent protein. Data is the mean ± SEM $n = 12$ cells (YFP), 13 cells (CaM-RhoA(DP)), 14 cells (CaRQ) and 12 cells (RhoA(DP)). Images are false colored. (For interpretation of the references to color in this figure legend, the reader is referred to the web version of the article.)

Blebbing cells tended to show motility that was less linear and faster than wild type cells (Fig. 1E and F). On average, blebbing cells (overexpressing CaM-RhoA or Rho(DP)) had linearity values of 0.030 ± 0.008 compared with 0.125 ± 0.025 (YFP) and 0.083 ± 0.027 (CaRQ) which were significant differences ($P = 0.001$ for YFP and $P = 0.054$ for CaRQ, n at least 12 cells). The average speed of blebbing

cells was $3.03 \pm 0.46\,\mu$m/min compared with $1.11 \pm 0.09\,\mu$m/min (YFP) and $1.73 \pm 0.12\,\mu$m/min (CaRQ) which were also significant differences ($P = 0.001$ for YFP and $P = 0.012$ for CaRQ). This shows that there are quantifiable differences in the motility characteristics between blebbing cells and those with wild type morphology.

3.2. CaM-RhoA(DP) fusion protein can switch characteristic cell migration characteristics

Delivering extracellular cues that switched intracellular Ca^{2+} increased the linearity and decreased the speed of motility of blebbing cells (Fig. 2). Chemicals such as ionomycin have been shown to abolish the blebbing morphology in cells overexpressing CaM-RhoA(DP) in a Ca^{2+}- and RhoA/ROCK-dependent manner previously [10]. Similarly, blue light (438 nm) has been shown to mediate bleb retraction in cells co-expressing CaM-RhoA(DP) and LOVS1K/Orai1, an engineered photoactivatable channel for Ca^{2+}-specific influx [20]. Switching cell morphology from blebbing to not blebbing using CaM-RhoA(DP) appeared to change the motility patterns and characteristics of centroid tracks of cells from a non-linear, jagged path to more straight, linear-like paths (Fig. 2A) when ionomycin was added half way through a 1 h time lapse experiment. It is important to note that ionomycin, at concentrations used in this work, did not affect cell viability within at least a 6 h interval (Supplemental Fig. 1). To quantify the time-dependence of this observed effect, the rolling average linearity and speed were calculated by considering a moving window of 5 time points (20 s of elapsed time).

Supplementary data related to this article found, in the online version, at http://dx.doi.org/10.1016/j.ceca.2012.12.005.

Linearity increased and speed decreased within minutes when blebbing cells overexpressing CaM-RhoA(DP) were stimulated with ionomycin (Fig. 2B and Movie 4). Within 2–3 min after ionomycin was added to cells, blebs retracted, as observed previously [10], and changes in motility closely coincided with morphology changes. After Ca^{2+} stimulation, the value of the rolling averages for linearity and speed approached those observed for wild type cells from above (Fig. 1). Those changes appeared to be somewhat reversible because the linearity and speed partially returned to initial values when the ionomycin-induced Ca^{2+} transient expired near the end of the experiments. Changes in morphology and motility speed and linearity were not observed when Ca^{2+} was absent from the extracellular space (Fig. 2B and D).

Supplementary data related to this article found, in the online version, at http://dx.doi.org/10.1016/j.ceca.2012.12.005.

Ca^{2+} can be delivered using a variety of Ca^{2+}-mobilizing modules, and illumination of cells co-expressing CaM-RhoA(DP) and LOVS1K/Orai1 also increased the linearity and decreased the speed of centroid shifts in those cells (Fig. 2C and D). LOVS1K is a recently reported chimera of the LOV2 domain from phototropin-1 fused to a soluble fragment of Stim1. On illumination, the LOV2-Stim1 fragment fusion (LOVS1K) associates with Orai1, mediating a local Ca^{2+} influx [20]. Changes in linearity and speed occurred gradually over 1 h, and became especially noticeable after 20–30 min of delivering 300 ms flashes of blue light every 10 s. The magnitude of the changes were more easily seen by comparing the average speed and linearity of cells in the first and second 30 min

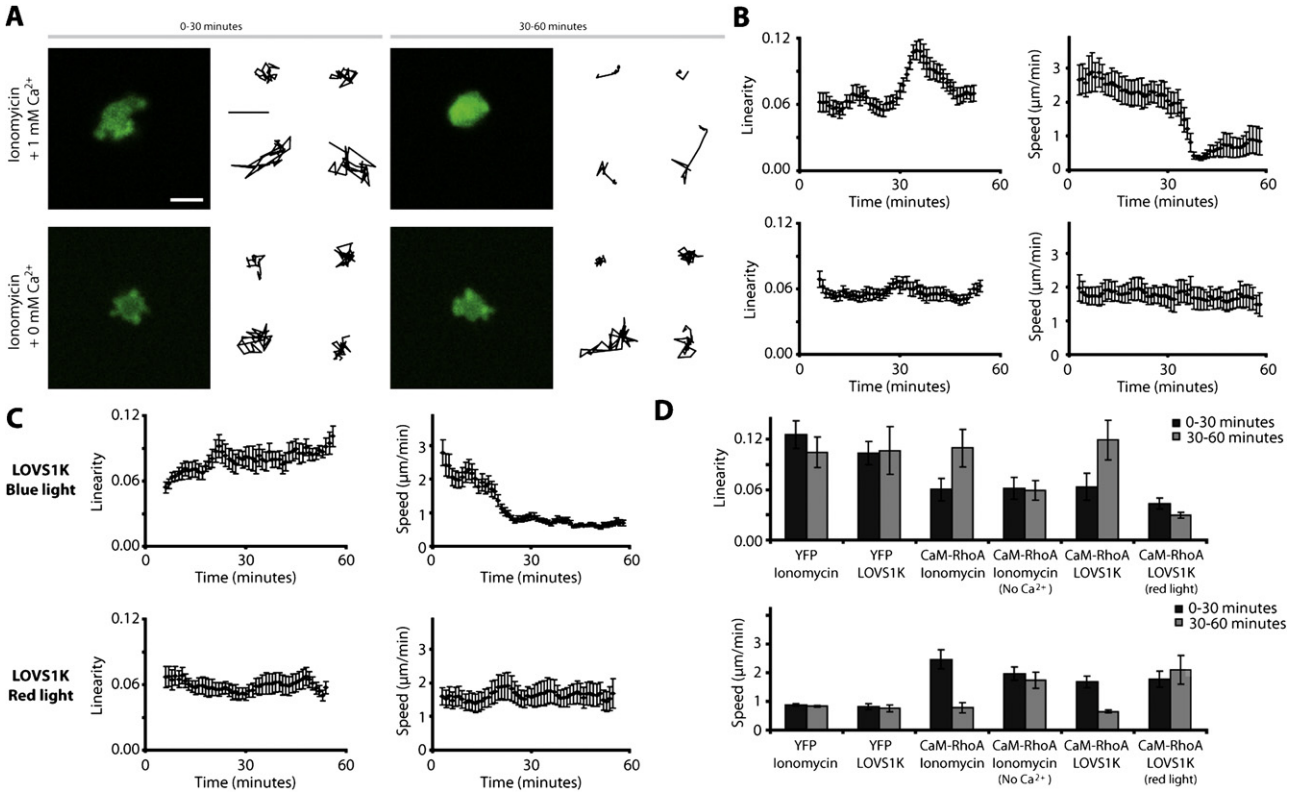

Fig. 2. Time-dependence of morphology and motility changes due to switching CaM-RhoA(DP). (A) Representative images of cells and tracks before (0–30 min) and after (30–60 min) ionomycin for cells in the presence (top) or absence (bottom) of Ca^{2+}. Scale bar is 20 μm in images and 10 μm in tracks. YFP channel is shown for each case. (B) Rolling average (over 20 s) of linearity and speed of CaM-RhoA(DP) cells in the presence (top) or absence (bottom) of Ca^{2+}, stimulated with ionomycin at 30 min. (C) Rolling average (over 20 s) of linearity and speed of CaM-RhoA(DP)/LOVS1K/Orai1 cells illuminated with blue light (top) or red light (bottom). (D) Summary of changes of in linearity and speed for cells presented in B and C, and control YFP expressing cells for the indicated conditions. Data in B–D are mean ± SEM, $n = 12$ cells (CaM-RhoA(DP) with ionomycin, both cases), 10 cells (CaM-RhoA(DP) with LOVS1K, both cases), 12 cells (YFP with LOVS1K) and 15 (YFP with ionomycin). Images are falsely colored. (For interpretation of the references to color in this figure legend, the reader is referred to the web version of the article.)

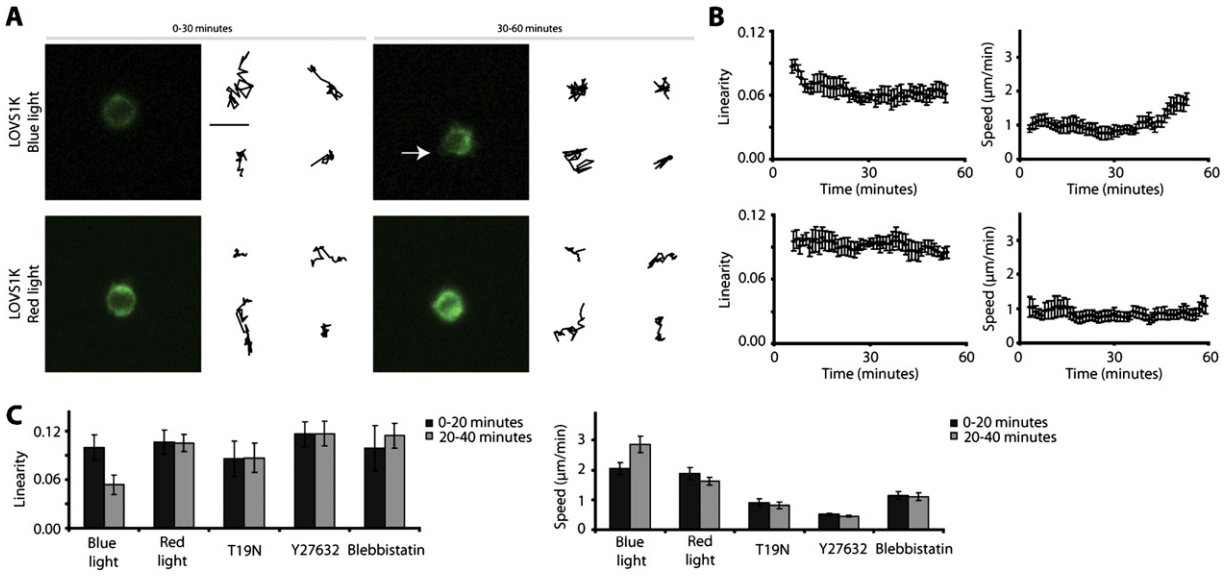

Fig. 3. Time-dependence of morphology and motility changes due to switching CaRQ. (A) Representative images of cells and tracks in the first 30 min and second 30 min of the experiment for cells co-expressing CaRQ and LOVS1K/Orai1 illuminated with blue light (top) and red light (bottom). Scale bar is 20 μm in images and 10 μm in tracks. YFP channel is shown for each case. (B) Rolling average (over 20 s) of linearity and speed of CaRQ/LOVS1K/Orai1 cells illuminated with blue light (top) or red light (bottom) throughout. Colored bars indicate duration and wavelength of light exposure. (C) Summary of changes of in linearity and speed for cells presented in A and B, and the indicated control conditions. Data in B–D are mean ± SEM. $n = 11$ cells (blue light and red light cases) and 10 cells (T19N, Y27632 and blebbistatin cases). Images are falsely colored. (For interpretation of the references to color in this figure legend, the reader is referred to the web version of the article.)

halves of the 1 h experiments (Fig. 2D). Unlike ionomycin, the Ca^{2+} influx of LOVS1K can be maintained for several hours, provided that light flashing is continued. No changes in morphology, migration or speed were observed when red light (580 nm) was delivered to cells; this wavelength of light does not cause conformational changes in the LOV2 domain that drives the Ca^{2+} influx of LOVS1K.

3.3. CaRQ fusion proteins can also switch cell migration characteristics

When cells co-expressing a PM-tagged version of CaRQ and LOVS1K/Orai1 were illuminated with blue light for 1 h, linearity decreased and speed increased, consistent with a morphology switch due to Ca^{2+} influx (Fig. 3 and Movie 5). Cell centroid tracks showed that cells tended to move in short, jagged paths in the second half of the experiment window compared to the more qualitatively linear tracks in the first half of the experiment (Fig. 3A). Considering the time course changes of linearity and speed over the 1 h experiment, linearity decreased mostly during the first 20 min, but the speed of centroid shifts did not increase until the last 20 min (Fig. 3B). In previous experiments with CaRQ and light-activated Ca^{2+} channels, morphology changes occurred gradually and tended to appear 10–30 min after the onset of illumination [11], and this agrees well with the observed timeframe for the reduction in linearity. With CaRQ/LOVS1K, blebbing became more likely and the blebs larger with increased illumination; the relationship between speed and morphology may require a large morphology change to become evident. When linearity and speed in the first 20 min portion and last 20 min portion of the experiment were compared, there were significant differences in speed and linearity ($P = 0.011$ and 0.029, $n = 12$ cells, respectively) (Fig. 3C).

Supplementary data related to this article found, in the online version, at http://dx.doi.org/10.1016/j.ceca.2012.12.005.

The changes in linearity and speed with illumination were dependent on the wavelength of light, RhoA activity and ROCK activity (Fig. 3C). When cells were illuminated with red light (580 nm), there were no significant changes in motility characteristics. The dominant negative RhoA mutation T19N [27], and pre-incubation with Y-27632 (a ROCK inhibitor) or blebbistatin (a myosin ATPase inhibitor) [13] also prevented any changes in speed or linearity occurring due to blue light illumination. Inhibition of RhoA or ROCK did not appear to have an effect on the linearity of wild type morphology cells, but they did reduce the speed at which those cells migrated during the imaging window both before and after illumination. This was expected because these experimental conditions inhibit cellular processes that regulate and execute cell movement.

3.4. Re-programmed cells migrate in response to blue light, ACh and VEGF-A

The experiments above demonstrate that single cell migration characteristics indicative of blebbing cells such as high migration speed and low linearity can be altered by switching the activity of engineered proteins. In the absence of any directional cue, however, blebbing cells appeared to undergo a random walk, as seen in the migration tracks (Figs. 1–3). Transwell migration assays could be used to present a directional cue to cells seeded on the apical side of the porous filter, with a partial chemical gradient established between the apical and basal chambers. We wanted to show that "re-programmed" cells could migrate in response to a variety of signals such as light, small molecules and peptides. Blue light and ACh have been shown to switch morphology changes mediated by CaRQ previously [11]; several growth factor receptors, such as EGFR [42] and VEGFR2 [18], generate Ca^{2+} transients as part of their downstream signaling, and their ligands may also be used to activate CaRQ.

VEGF-A/VEGFR2-induced Ca^{2+} transients were able to activate CaRQ blebbing (Fig. 4). The VEGFR2 gene was fused with YFP (Fig. 4A) and VEGF-A elicited a Ca^{2+} transient, measured with the TN-XL biosensor [43], when VEGFR2-YFP was expressed (Fig. 4B). While both the TN-XL biosensor and VEGFR2 were fused with YFP, the YFP associated with VEGFR2 was minimally activated by the CFP excitation light used to measure the TN-XL biosensor (FRET effects fall of quickly with distance between fluorescent proteins) and

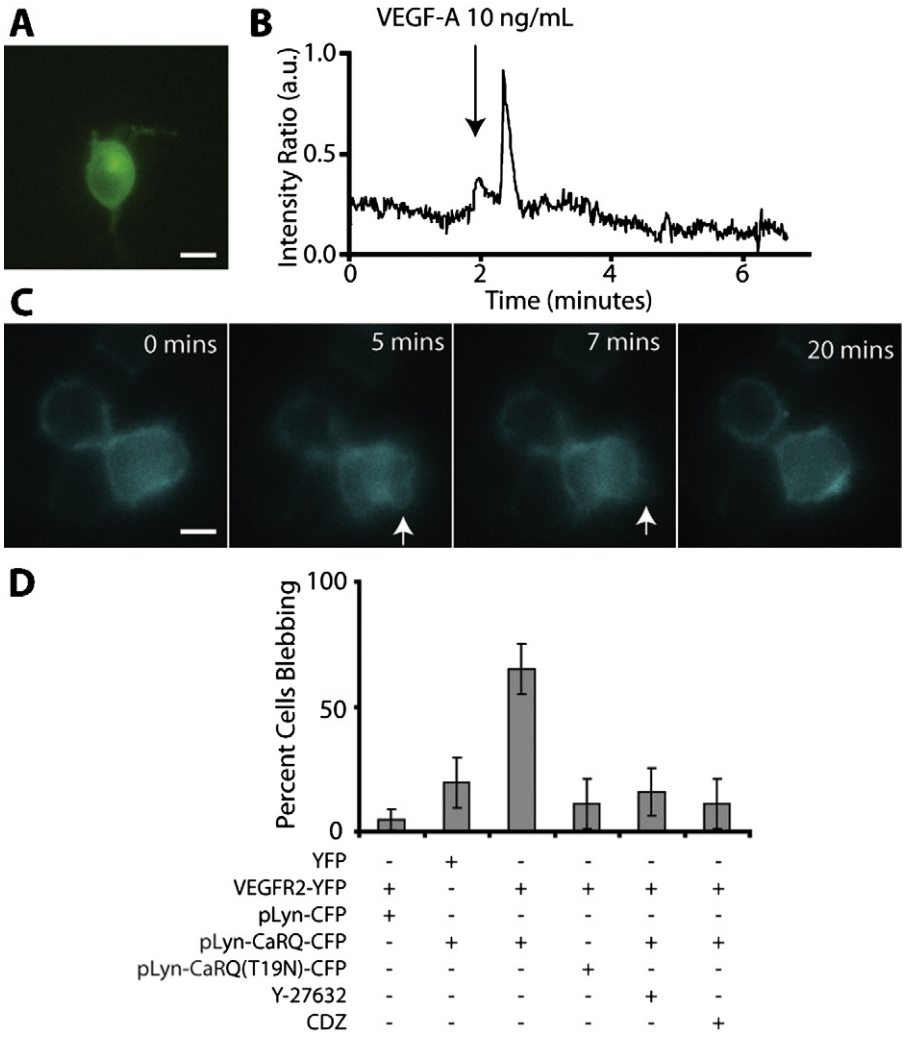

Fig. 4. VEGFR2 is a Ca^{2+}-mobilizing module that activated CaRQ. (A) Fluorescence image of VEGFR2-YFP in HEK293 cells. (B) Ratio of YFP/CFP intensities of TNXL Ca^{2+} biosensor in cells expressing VEGFR2-YFP. (C) CFP images of HEK293 cells co-expressing pLyn-CaRQ-CFP and VEGFR2-YFP stimulated with 5 ng/mL VEGF-A at 5 min in Ca^{2+}-PBS. White arrow heads show blebs and scale bars in A and C are 10 μm. (D) Percent of cells blebbing after VEGF-A stimulation in the indicated condition. Data is mean ± standard deviation, $n = 3$ independent experiments. Images are falsely colored. (For interpretation of the references to color in this figure legend, the reader is referred to the web version of the article.)

some bleed through would not substantially affect our qualitative observations. The Ca^{2+} transient recorded was similar in amplitude, shape and duration to those reported in the literature [18]. The Ca^{2+} transient due to VEGF-A/VEGFR2 was similar to others used as Ca^{2+}-mobilizing modules in our previous work [10,11], suggesting that VEGFR2 may also be used as a Ca^{2+}-mobilizing module where VEGF-A is the input chemical signal.

VEGF-A stimulation resulted in bleb formation when VEGFR2-YFP and CaRQ-CFP were co-expressed (Fig. 4C and D). Bleb formation began 2–3 min after 10 ng/mL VEGF-A was added to Ca^{2+}-PBS. Blebbing lasted for approximately 5 min in most cells observed. Blebbing was abrogated by pre-incubation of cells with the CaM inhibitor calmidazolium (CDZ) or Y-27632. Similarly, stimulation of cells expressing the dominant negative mutation, CaRQ(T19N)-CFP with VEGFR2 or CaRQ-CFP alone did not cause blebbing. This showed that VEGFR2 is a Ca^{2+}-mobilizing module capable of CaRQ activation.

Cells co-expressing CaRQ and LOVS1K/Orai1 or VEGFR2 or nAChR-α4 Ca^{2+} mobilizing modules showed increased likelihood to migrate through porous filters in transwell assays when stimulated with light, VEGF-A or ACh, respectively (Fig. 5). Transwell assays were used to test population-level migration rather than wound assays because wound assays are more difficult to analyze without bias and present soluble migration cues. Migration was reported as the migration index, the ratio of number of migrated cells after 24 h to the number of cells in a positive control well (see Section 2 for more details). The migration index ranges from 0 to 1 where 0 indicates that no cells migrated through the porous filter and 1 indicates that all seeded cells migrated. For LOVS1K/Orai1, blue light was shone on the transwell inserts from below such that the light traveled approximately parallel to the direction of migration through the porous inserts; for VEGF-A and ACh, these stimuli were added to the basal chamber only (Fig. 5A).

The average migration index for CaRQ cells co-expressing LOVS1K/Orai1 was 0.53 ± 0.02, for VEGFR2 it was 0.50 ± 0.10 and for nAChR-α4 it was 0.42 ± 0.05, when stimulated with the appropriate conditions. For CaRQ(T19N) the migration indices under those same conditions were 0.07 ± 0.02, 0.07 ± 0.04 and 0.04 ± 0.04, which were significantly different than the dominant positive mutants ($P < 0.001$, $P = 0.029$ and $P = 0.003$, $n = 3$ experiments), and were similar for other control conditions such ROCK inhibition (by Y-27632 treatment) or when no stimulus was provided. The transwell assay is not a perfect model of migration of cells toward a source because chemical concentration gradients cannot be maintained

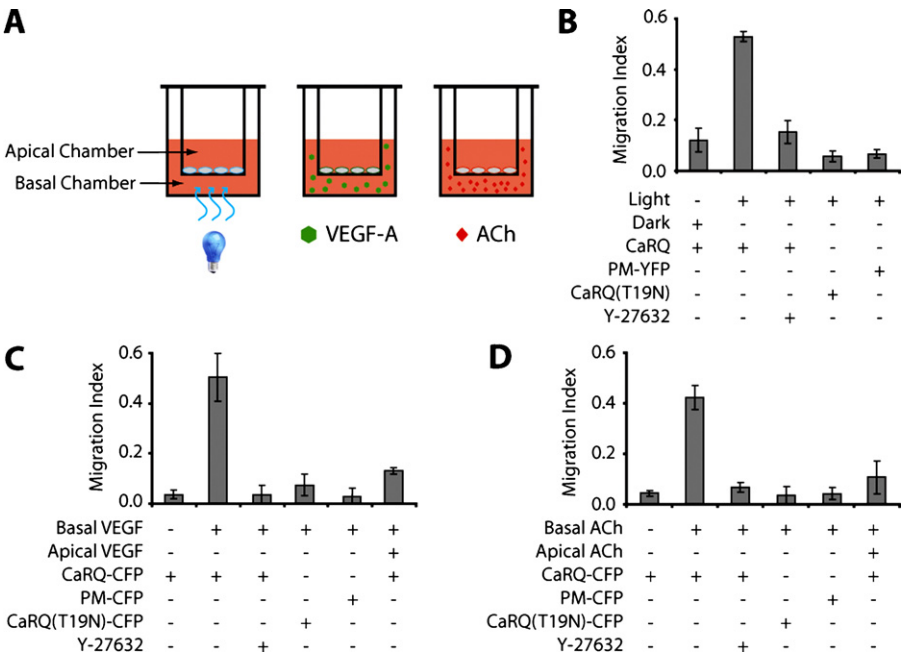

Fig. 5. Multi-signal migration of CaRQ-expressing cells using transwell assays. (A) Schematic cartoon of the three different setups used to stimulate CaRQ cells. (B–D) Migration index of cells using the transwell assays for the indicated conditions. For all three cases, the Ca^{2+}-mobilizing module was transfected in all cells (B, LOVS1K/Orai1; C, VEGFR2; D, nAChR-α4). The data is the mean ± standard deviation, $n = 3$ independent experiments.

indefinitely. However, the condition where chemicals (VEGF-A or ACh) were present in both the apical and basal chambers showed that the chemical gradient is a significant contribution toward the migration of the re-programmed cells.

Non-adherent cells co-expressing CaRQ, LOVS1K and Orai1, illuminated primarily on one side, moved in a direction that was generally toward the light source (Fig. 6). To achieve a clear, single-cell readout of the ability of our synthetic protein network to control directed cell migration, a simple light pattern was established using an objective lens with a restricted light aperture such that the light source was located near one side of the cell while the other side of the cell was exposed to darkness, conceptually similar to what has been achieved with a pharmacological approach before [44]. Jurkat cells were used because they are non-adherent, and so we reasoned that their migration *in vitro* would be greater than similarly stimulated adherent cells. Indeed, Jurkat cells co-expressing CaRQ, LOVS1K and Orai1 tended to form blebs on the side of the cell closer to the light source (Fig. 6A) and generally moved toward the light source (Fig. 6B). Cells co-expressing CaRQ(T19N), LOVS1K and Orai1 did not exhibit any observable morphology changes or migration (Fig. 6C and D).

4. Discussion

Here we have shown that cells can be re-programmed to change their motility and migration, using engineered proteins, by manipulating RhoA, and, given the above control experiments, the blebbing morphology. Blebbing has generally been studied in 3D environments (*in vivo* [21,22] or in thick gel invasion assays [24,25]), however here we show that blebbing can affect motility characteristics such as speed and linearity in 2D environments. Analyzing these characteristics of cells may help to objectively identify their morphology and migration mode, which may provide a new way of categorizing cell types (*e.g.* primary cancer cells) with clinical relevance. Blebbing cell tracks showed jagged, chaotic movement in our experiments, even though *in vivo*, blebbing can mediate directed cell migration [21]. In our experiments, since there was no directional cue, blebbing cells can undergo a random walk. Another cause for the chaotic centroid shifts may have been a reduced ability to translate tumbling forward into traction forces. E-cadherin has been implicated in anchoring blebbing cells to their neighboring cells during the aging and retraction of a bleb, which allows the cytoskeletal tension and "tumble forward" to be translated into traction forces and incremental migration [22]. The mechanism that helps to anchor blebbing cells during their tumble forward in 2D migration is yet to be elucidated, although some kind of transmembrane adhesion receptor such as cadherins or integrins are likely involved.

We used the centroid of a cell to calculate its position, speed and linearity and report its tracks. The centroid is the arithmetic average of pixel positions, where x and y coordinates are calculated independently, and there is no weighting for pixel intensity above a set threshold (see Section 2 for more details). One limitation of this method is that it does not fully account for changes in cell morphology due to the formation and retraction of a bleb. However, for most cells the size of the bleb relative to cell body was too small to make a noticeable difference in the calculated centroid of the cell compared to translation of the cell body. While we have used these methods to characterize the behavior of our engineered cells, the methods may be applicable to studying factors affecting morphology and migration of blebbing cells in 2D environments, such as the role of specific intracellular proteins or the effect of environmental factors like substrate adhesion or soluble chemicals, on motility and migration.

Activation of RhoA, and the established subsequent blebbing morphology increased the likelihood of cell migration in transwell assays. Initially, this appears to be in contrast to the generally accepted notion that over-expression of dominant positive Rho proteins inhibits cell migration [45,46]. However, in this case activation of CaRQ, therefore dominant positive RhoA, resulted in blebbing in cells, a morphology that has been directly linked to increased cell motility in development [21,22] and cancer cells [24,25]. Direct activation or inactivation of RhoA leading to changes in blebbing-associated migration, to our knowledge, has not been shown previously to affect cell migration. However, inhibition of RhoGEF's [24] and inactivation of ROCK [15,16] is known to directly

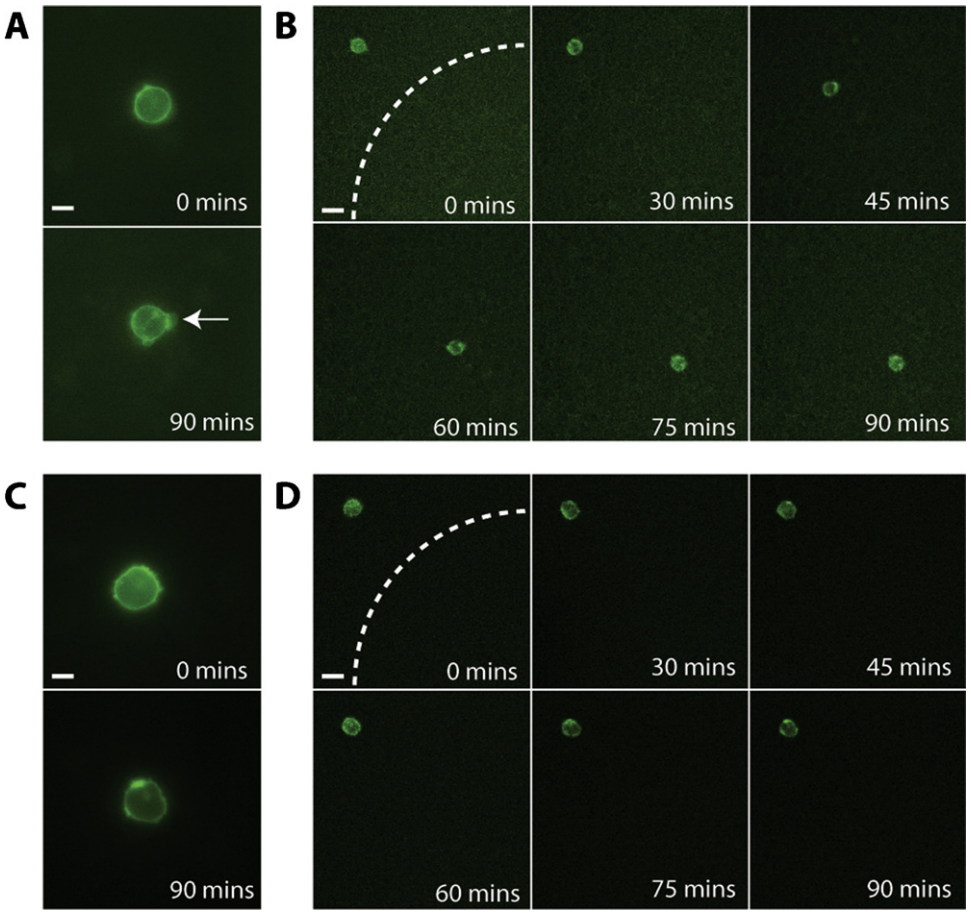

Fig. 6. Directed migration of CaRQ-expressing cells in response to a directional light signal. (A) High magnification images of Jurkat cells co-expressing CaRQ, LOVS1K and Orai1 (CaRQ/YFP channel shown) before (top) and after (bottom) illumination. White arrow indicates new blebs. (B) Lower magnification images of the cell in A during the 90 min time course, showing the change in cell position over time. The light source was situated in the lower right corner of the field of view (see E). (C, D) Analogous images are presented as in A and B, respectively, for cells co-expressing CaRQ(T19N), LOVS1K and Orai1. YFP channel is shown in all images. Dashed lines in B and D denote the size and location of the blue light illumination pattern (illumination below and to the right of the dashed line). Scale bars in A and C are 10 μm and in B and D are 25 μm. Images are falsely colored and are representative of 3 experiments for each case. (For interpretation of the references to color in this figure legend, the reader is referred to the web version of the article.)

affect blebbing and migration. Therefore, the result that RhoA can also affect morphology and migration in this mode was logical.

For single cell experiments, blue light was primarily used as the stimulus and LOVS1K/Orai1 as the Ca^{2+}-mobilizing module because light can be controlled more easily than chemicals in solution. In the transwell assays where a concentration gradient could be maintained for some time ACh and VEGF-A stimuli was used with nAChR-α4 and VEGFR2 as the Ca^{2+}-mobilizing domains to direct cell migration in addition to blue light/LOVS1K. The low level of "background" migration of HEK293 cells expressing VEGFR2 in the absence of CaRQ is likely due to a lack of specialized scaffolding and adapter proteins that are normally associated with VEGFR2, but were not introduced by transfection. For example, the phosphorylated adapter Gab1 has been shown to be required to be co-expressed with VEGFR2 in some cell lines, including HEK293, in order for VEGF signaling to robustly initiate migration [47,48]. VEGFR2 was able to generate a Ca^{2+} transient in these cells likely because PLC-γ, the protein that initiates the IP_3 cascade leading to Ca^{2+} mobilization [18], is endogenously present in HEK293 [49]. In experiments where stimulants were added to both the apical and basal chambers, cell migration was not significantly different than the other control conditions, suggesting that the directionality of the inducing signal is important to guide cell migration.

Experiments in Jurkat cells showed that cells tended to form blebs on the side of the cell that was most exposed to stimulus, in this case, blue light. Further, cells tended to migrate in the direction of the light stimulus, and therefore, in the direction of dynamically forming blebs. The illumination pattern created a distinct "light" and "dark" region (Fig. 6B and D); there was likely light scattering through the culture medium which resulted in a partial gradient-like zone between the two regions that may have accounted to for some of the direction migration. Migration toward the side of bleb formation is consistent with *in vivo* reports of blebbing-based migration, where, for example, cells have been shown to migration along a CXCR4 gradient in *D. Rerio* [21].

The Ca^{2+} second messenger was used as an intermediate to translate extracellular signals into morphology changes and migration in this study. We have used Ca^{2+} and CaM extensively to engineer a variety of proteins including translocation assays and morphology switches [10,11,50,51] because Ca^{2+} is easy to deliver and monitor, and is an inherently modular signaling component. The wide applicability of the Ca^{2+} signal may appear to be a weakness of our approach given the many cellular processes regulated by Ca^{2+}; yet cells are not confused by the interpretation of a Ca^{2+} signal in nature. The specific response to a Ca^{2+} signal is naturally tailored by the spatiotemporal properties of the Ca^{2+} signal (*e.g.* subcellular localization, concentration level, frequency and duration) as well as the reconfiguration of a large toolbox of proteins that respond to and transport Ca^{2+} [17]. With the engineered Ca^{2+}-responsive systems here, where Ca^{2+}-mobilization and Ca^{2+}-response have been

purposefully coordinated in time and space, the specific response to the Ca^{2+} signal can be re-defined.

Our demonstration that CaRQ can regulate cell migration is an important contribution to cell programming because it shows that control over cell motility and migration can be rewired in a flexible and tunable way. Control over cell migration could be applicable to many programming applications such as guiding cells to populate a biomaterial scaffold or microfluidic device, or targeting cells to sites of injury or disease *in vivo*. Other strategies have developed light-based control of cell migration previously [9,13], however CaRQ has the unique ability to regulate blebbing and therefore control the amoeboid-like cell migration mode. The ability to control cell migration with multiple signal inputs is a new feature not offered by existing cell migration control strategies. Previous systems designed using specific caging mechanisms [13] and protein–protein interactions [9] rely on specific wavelengths of light to activate Rho GTPases. The strategy presented in this work shows how two modules can be combined to achieve control by light or chemical signals. The use of exogenous chemicals to control cell migration may make CaRQ more suitable for controlling cell migration *in vivo* in large organisms with poor light penetration.

5. Conclusion

The relationship between cell morphology (*i.e.* blebbing) and cell migration characteristics was qualified by analyzing parameters such as speed and linearity. The speed and linearity of cells was switched using engineered, Ca^{2+}-responsive Rho proteins and through this, cells were re-programmed to migrate in response to a variety of extracellular signals including blue light, ACh and VEGF-A. This demonstrates that spatiotemporal control of RhoA can re-program the motility patterns and migration of living cells using amoeboid-like migration. The analysis developed here may be used to characterize and study the migratory phenotypes of different types of cells (such as primary cancer cells) based on their environment-dependent and genetic differences.

Authors' contributions

EM designed and carried out all experiments, analyzed the data and wrote the manuscript. KT provided guidance and helped write the manuscript.

Acknowledgements

This work was made possible by plasmid sharing through Addgene. This work was supported by a fellowship to EM from the Natural Science and Engineering Research Council and a grant to KT from the Canadian Institutes of Health Research (#81262).

References

[1] C.J. Breitbach, J. Burke, D. Jonker, J. Stephenson, A.R. Haas, L.Q. Chow, J. Nieva, T.H. Hwang, A. Moon, R. Patt, et al., Intravenous delivery of a multi-mechanistic cancer-targeted oncolytic poxvirus in humans, Nature 477 (2011) 99–102.
[2] M. Kalos, B.L. Levine, D.L. Porter, S. Katz, S.A. Grupp, A. Bagg, C.H. June, T cells with chimeric antigen receptors have potent antitumor effects and can establish memory in patients with advanced leukemia, Science Translational Medicine 3 (2011), 95ra73.
[3] M. Kamata, S. Liu, M. Liang, Y. Nagaoka, I.S. Chen, Generation of human induced pluripotent stem cells bearing an anti-HIV transgene by a lentiviral vector carrying an internal murine leukemia virus promoter, Human Gene Therapy 21 (2010) 1555–1567.
[4] R.A. Petros, J.M. DeSimone, Strategies in the design of nanoparticles for therapeutic applications, Nature Reviews Drug Discovery 9 (2010) 615–627.
[5] J.A. Hubbell, S.N. Thomas, M.A. Swartz, Materials engineering for immunomodulation, Nature 462 (2009) 449–460.
[6] W. Weber, M. Fussenegger, Engineering of synthetic mammalian gene networks, Chemistry and Biology 16 (2009) 287–297.
[7] A. Hall, Rho GTPases and the actin cytoskeleton, Science 279 (1998) 509–514.
[8] D.W. Leung, C. Otomo, J. Chory, M.K. Rosen, Genetically encoded photoswitching of actin assembly through the Cdc42-WASP-Arp2/3 complex pathway, Proceedings of the National Academy of Sciences of the United States of America 105 (2008) 12797–12802.
[9] A. Levskaya, O.D. Weiner, W.A. Lim, C.A. Voigt, Spatiotemporal control of cell signalling using a light-switchable protein interaction, Nature 461 (2009) 997–1001.
[10] E. Mills, E. Pham, K. Truong, Structure based design of a Ca^{2+}-sensitive RhoA protein that controls cell morphology, Cell Calcium 48 (2010) 195–201.
[11] E. Mills, K. Truong, Ca(2+)-mediated synthetic biosystems offer protein design versatility, signal specificity, and pathway rewiring, Chemistry and Biology 18 (2011) 1611–1619.
[12] X. Wang, L. He, Y.I. Wu, K.M. Hahn, D.J. Montell, Light-mediated activation reveals a key role for Rac in collective guidance of cell movement in vivo, Nature Cell Biology 12 (2010) 591–597.
[13] Y.I. Wu, D. Frey, O.I. Lungu, A. Jaehrig, I. Schlichting, B. Kuhlman, K.M. Hahn, A genetically encoded photoactivatable Rac controls the motility of living cells, Nature 461 (2009) 104–108.
[14] B.J. Yeh, R.J. Rutigliano, A. Deb, D. Bar-Sagi, W.A. Lim, Rewiring cellular morphology pathways with synthetic guanine nucleotide exchange factors, Nature 447 (2007) 596–600.
[15] G. Charras, E. Paluch, Blebs lead the way: how to migrate without lamellipodia, Nature Reviews Molecular Cell Biology 9 (2008) 730–736.
[16] O.T. Fackler, R. Grosse, Cell motility through plasma membrane blebbing, Journal of Cell Biology 181 (2008) 879–884.
[17] M.J. Berridge, P. Lipp, M.D. Bootman, The versatility and universality of calcium signalling, Nature Reviews Molecular Cell Biology 1 (2000) 11–21.
[18] N.S. Dawson, D.C. Zawieja, M.H. Wu, H.J. Granger, Signaling pathways mediating VEGF165-induced calcium transients and membrane depolarization in human endothelial cells, FASEB Journal 20 (2006) 991–993.
[19] R. Nashmi, M.E. Dickinson, S. McKinney, M. Jareb, C. Labarca, S.E. Fraser, H.A. Lester, Assembly of alpha4beta2 nicotinic acetylcholine receptors assessed with functional fluorescently labeled subunits: effects of localization, trafficking, and nicotine-induced upregulation in clonal mammalian cells and in cultured midbrain neurons, Journal of Neuroscience 23 (2003) 11554–11567.
[20] E. Pham, E. Mills, K. Truong, A synthetic photoactivated protein to generate local or global Ca(2+) signals, Chemistry and Biology 18 (2011) 880–890.
[21] H. Blaser, M. Reichman-Fried, I. Castanon, K. Dumstrei, F.L. Marlow, K. Kawakami, L. Solnica-Krezel, C.P. Heisenberg, E. Raz, Migration of zebrafish primordial germ cells: a role for myosin contraction and cytoplasmic flow, Developmental Cell 11 (2006) 613–627.
[22] E. Kardash, M. Reichman-Fried, J.L. Maitre, B. Boldajipour, E. Papusheva, E.M. Messerschmidt, C.P. Heisenberg, E. Raz, A role for Rho GTPases and cell-cell adhesion in single-cell motility in vivo, Nature Cell Biology 12 (2010) 47–53, suppl. pp. 1–11.
[23] T. Lammermann, B.L. Bader, S.J. Monkley, T. Worbs, R. Wedlich-Soldner, K. Hirsch, M. Keller, R. Forster, D.R. Critchley, R. Fassler, et al., Rapid leukocyte migration by integrin-independent flowing and squeezing, Nature 453 (2008) 51–55.
[24] E. Sahai, C.J. Marshall, Differing modes of tumour cell invasion have distinct requirements for Rho/ROCK signalling and extracellular proteolysis, Nature Cell Biology 5 (2003) 711–719.
[25] V. Sanz-Moreno, G. Gadea, J. Ahn, H. Paterson, P. Marra, S. Pinner, E. Sahai, C.J. Marshall, Rac activation and inactivation control plasticity of tumor cell movement, Cell 135 (2008) 510–523.
[26] Z. Chen, D. Borek, S.B. Padrick, T.S. Gomez, Z. Metlagel, A.M. Ismail, J. Umetani, D.D. Billadeau, Z. Otwinowski, M.K. Rosen, Structure and control of the actin regulatory WAVE complex, Nature 468 (2010) 533–538.
[27] O. Pertz, L. Hodgson, R.L. Klemke, K.M. Hahn, Spatiotemporal dynamics of RhoA activity in migrating cells, Nature 440 (2006) 1069–1072.
[28] M.E. Ward, J.Y. Wu, Y. Rao, Visualization of spatially and temporally regulated N-WASP activity during cytoskeletal reorganization in living cells, Proceedings of the National Academy of Sciences of the United States of America 101 (2004) 970–974.
[29] R.A. Worthylake, S. Lemoine, J.M. Watson, K. Burridge, RhoA is required for monocyte tail retraction during transendothelial migration, Journal of Cell Biology 154 (2001) 147–160.
[30] G.T. Charras, C.K. Hu, M. Coughlin, T.J. Mitchison, Reassembly of contractile actin cortex in cell blebs, Journal of Cell Biology 175 (2006) 477–490.
[31] C. Cantarella, L. Sepe, F. Fioretti, M.C. Ferrari, G. Paolella, Analysis and modelling of motility of cell populations with MotoCell, BMC Bioinformatics 10 (Suppl. 12) (2009) S12.
[32] M. Reichman-Fried, S. Minina, E. Raz, Autonomous modes of behavior in primordial germ cell migration, Developmental Cell 6 (2004) 589–596.
[33] L.P. Desai, A.M. Aryal, B. Ceacareanu, A. Hassid, C.M. Waters, RhoA and Rac1 are both required for efficient wound closure of airway epithelial cells, American Journal of Physiology Lung Cellular and Molecular Physiology 287 (2004) L1134–L1144.
[34] M. Hirakawa, Y. Karashima, M. Watanabe, C. Kimura, Y. Ito, M. Oike, Protein kinase A inhibits lysophosphatidic acid-induced migration of airway smooth muscle cells, Journal of Pharmacology and Experimental Therapeutics 321 (2007) 1102–1108.
[35] C.C. Liang, A.Y. Park, J.L. Guan, In vitro scratch assay: a convenient and inexpensive method for analysis of cell migration in vitro, Nature Protocols 2 (2007) 329–333.

[36] D. Rosel, J. Brabek, O. Tolde, C.T. Mierke, D.P. Zitterbart, C. Raupach, K. Bicanova, P. Kollmannsberger, D. Pankova, P. Vesely, et al., Up-regulation of Rho/ROCK signaling in sarcoma cells drives invasion and increased generation of protrusive forces, Molecular Cancer Research 6 (2008) 1410–1420.
[37] R. Torka, F. Thuma, V. Herzog, G. Kirfel, ROCK signaling mediates the adoption of different modes of migration and invasion in human mammary epithelial tumor cells, Experimental Cell Research 312 (2006) 3857–3871.
[38] R.A. Worthylake, K. Burridge, RhoA and ROCK promote migration by limiting membrane protrusions, Journal of Biological Chemistry 278 (2003) 13578–13584.
[39] F.M. Vega, G. Fruhwirth, T. Ng, A.J. Ridley, RhoA and RhoC have distinct roles in migration and invasion by acting through different targets, Journal of Cell Biology 193 (2011) 655–665.
[40] M. Veronika, R. Welsch, A. Ng, P. Matsudaira, J.C. Rajapakse, Correlation of cell membrane dynamics and cell motility, BMC Bioinformatics 12 (Suppl. 13) (2011) S19.
[41] J.Y. Tinevez, U. Schulze, G. Salbreux, J. Roensch, J.F. Joanny, E. Paluch, Role of cortical tension in bleb growth, Proceedings of the National Academy of Sciences of the United States of America 106 (2009) 18581–18586.
[42] I. Tinhofer, K. Maly, P. Dietl, F. Hochholdinger, S. Mayr, A. Obermeier, H.H. Grunicke, Differential Ca^{2+} signaling induced by activation of the epidermal growth factor and nerve growth factor receptors, Journal of Biological Chemistry 271 (1996) 30505–30509.
[43] M. Mank, D.F. Reiff, N. Heim, M.W. Friedrich, A. Borst, O. Griesbeck, A FRET-based calcium biosensor with fast signal kinetics and high fluorescence change, Biophysical Journal 90 (2006) 1790–1796.
[44] P.T. Yam, C.A. Wilson, L. Ji, B. Hebert, E.L. Barnhart, N.A. Dye, P.W. Wiseman, G. Danuser, J.A. Theriot, Actin–myosin network reorganization breaks symmetry at the cell rear to spontaneously initiate polarized cell motility, Journal of Cell Biology 178 (2007) 1207–1221.
[45] A. Panopoulos, M. Howell, R. Fotedar, R.L. Margolis, Glioblastoma motility occurs in the absence of actin polymer, Molecular Biology of the Cell 22 (2011) 2212–2220.
[46] J. Xu, F. Wang, A. Van Keymeulen, P. Herzmark, A. Straight, K. Kelly, Y. Takuwa, N. Sugimoto, T. Mitchison, H.R. Bourne, Divergent signals and cytoskeletal assemblies regulate self-organizing polarity in neutrophils, Cell 114 (2003) 201–214.
[47] K. Holmes, O.L. Roberts, A.M. Thomas, M.J. Cross, Vascular endothelial growth factor receptor-2: structure, function, intracellular signalling and therapeutic inhibition, Cellular Signalling 19 (2007) 2003–2012.
[48] M. Laramee, C. Chabot, M. Cloutier, R. Stenne, M. Holgado-Madruga, A.J. Wong, I. Royal, The scaffolding adapter Gab1 mediates vascular endothelial growth factor signaling and is required for endothelial cell migration and capillary formation, Journal of Biological Chemistry 282 (2007) 7758–7769.
[49] B.K. Atwood, J. Lopez, J. Wager-Miller, K. Mackie, A. Straiker, Expression of G protein-coupled receptors and related proteins in HEK293, AtT20, BV2, and N18 cell lines as revealed by microarray analysis, BMC Genomics 12 (2011) 14.
[50] E. Mills, K. Truong, Rate and extent of protein localization is controlled by peptide-binding domain association kinetics and morphology, Protein Science 18 (2009) 1252–1260.
[51] E. Mills, K. Truong, Engineering Ca^{2+}/calmodulin-mediated modulation of protein translocation by overlapping binding and signaling peptide sequences, Cell Calcium 47 (2010) 369–377.
[52] D.F. Silva, R.A. Mesquita-Ferrari, K.P. Fernandes, M.P. Raele, N.U. Wetter, A.M. Deana, Effective transmission of light for media culture, plates and tubes, Photochemistry and Photobiology 88 (2012) 1211–1216.